1-1-2014

Magnetic phase transitions and entropy change in layered NdMn1.7Cr0.3Si2

M F. Md Din
University of Wollongong, mfmd999@uowmail.edu.au

Jianli Wang
University of Wollongong, jianli@uow.edu.au

S J. Campbell
University of New South Wales, stewart.campbell@adfa.edu.au

A J. Studer
ANSTO

M Avdeev
ANSTO

See next page for additional authors

Magnetic phase transitions and entropy change in layered NdMn1.7Cr0.3Si2

Abstract

A giant magnetocaloric effect has been observed around the Curie temperature, TC ∼ 42 K, in NdMn1.7Cr0.3Si2 with no discernible thermal and magnetic hysteresis losses. Below 400 K, three magnetic phase transitions take place around 380 K, 320 K and 42 K. Detailed high resolution synchrotron and neutron powder diffraction (10-400 K) confirmed the magnetic transitions and phases as follows: TN intra ∼ 380 K denotes the transition from paramagnetism to intralayer antiferromagnetism (AFI), TN inter ∼ 320 K represents the transition from the AFI structure to the canted antiferromagnetic spin structure (AFmc), while TC ∼ 42 K denotes the first order magnetic transition from AFmc to canted ferromagnetism (Fmc + F(Nd)) due to ordering of the Mn and Nd sub-lattices. The maximum values of the magnetic entropy change and the adiabatic temperature change, around TC for a field change of 5 T are evaluated to be −ΔSM max ∼ 15.9 J kg−1 K−1 and ΔTad max ∼ 5 K, respectively. The first order magnetic transition associated with the low levels of hysteresis losses (thermal

Keywords

3si2, 7cr0, magnetic, transitions, phase, change, entropy, layered, ndmn1

Disciplines

Engineering | Physical Sciences and Mathematics

Publication Details

Md Din, M. F., Wang, J. L., Campbell, S. J., Studer, A. J., Avdeev, M., Kennedy, S. J., Gu, Q. F., Zeng, R. & Dou, S. X. (2014). Magnetic phase transitions and entropy change in layered NdMn1.7Cr0.3Si2. Applied Physics Letters, 104 (4), 042401-1-042401-5.

Authors

M F. Md Din, Jianli Wang, S J. Campbell, A J. Studer, M Avdeev, S J. Kennedy, Q F. Gu, R Zeng, and S X. Dou

Magnetic phase transitions and entropy change in layered $NdMn_{1.7}Cr_{0.3}Si_2$

M. F. Md Din,[1,a)] J. L. Wang,[1,2] S. J. Campbell,[3] A. J. Studer,[2] M. Avdeev,[2] S. J. Kennedy,[2] Q. F. Gu,[4] R. Zeng,[1,5] and S. X. Dou[1]
[1]*Institute for Superconductivity and Electronic Materials, University of Wollongong, Wollongong, New South Wales 2522, Australia*
[2]*Bragg Institute, Australian Nuclear Science and Technology Organization, Lucas Heights, New South Wales 2234, Australia*
[3]*School of Physical, Environmental, and Mathematical Sciences, The University of New South Wales, Canberra, The Australian Defence Force Academy, Australian Capital Territory 2600, Australia*
[4]*Australian Synchrotron, 800 Blackburn Rd, Clayton 3168, Australia*
[5]*Solar Energy Technologies, School of Computing, Engineering and Mathematics, University of Western Sydney, Penrith, NSW 2751, Australia*

(Received 19 October 2013; accepted 3 January 2014; published online 27 January 2014)

A giant magnetocaloric effect has been observed around the Curie temperature, $T_C \sim 42$ K, in $NdMn_{1.7}Cr_{0.3}Si_2$ with no discernible thermal and magnetic hysteresis losses. Below 400 K, three magnetic phase transitions take place around 380 K, 320 K and 42 K. Detailed high resolution synchrotron and neutron powder diffraction (10–400 K) confirmed the magnetic transitions and phases as follows: $T_N^{intra} \sim 380$ K denotes the transition from paramagnetism to intralayer antiferromagnetism (AF*l*), $T_N^{inter} \sim 320$ K represents the transition from the AF*l* structure to the canted antiferromagnetic spin structure (AF*mc*), while $T_C \sim 42$ K denotes the first order magnetic transition from AF*mc* to canted ferromagnetism (F*mc* + F(Nd)) due to ordering of the Mn and Nd sub-lattices. The maximum values of the magnetic entropy change and the adiabatic temperature change, around T_C for a field change of 5 T are evaluated to be $-\Delta S_M^{max} \sim 15.9$ J kg^{-1} K^{-1} and $\Delta T_{ad}^{max} \sim 5$ K, respectively. The first order magnetic transition associated with the low levels of hysteresis losses (thermal $<\sim 0.8$ K; magnetic field $<\sim 0.1$ T) in $NdMn_{1.7}Cr_{0.3}Si_2$ offers potential as a candidate for magnetic refrigerator applications in the temperature region below 45 K. © *2014 AIP Publishing LLC*. [http://dx.doi.org/10.1063/1.4863230]

The continuing impact of global warming is offset in part by the use of environmentally friendly technologies with magnetic cooling based on the magnetocaloric effect (MCE) potentially advantageous in this regard. Harnessing the advantages of the MCE offers a relatively environmentally friendly and energy-efficient refrigeration mechanism which is expected to be the basis of an important cooling technology for the future.[1] A giant MCE is commonly observed in materials with a first order magnetic transition (FOMT), but such transitions are usually accompanied by thermal and magnetic hysteresis effects, thus diminishing the magnetic refrigerator performance.[2]

Ternary rare-earth (R) compounds of the type RT_2X_2, where T = transition metal and X = Si, Ge, exhibit a large variety of structural and physical properties (e.g., Refs. 3 and 4) and as such continue to attract interest. The interplay between the R-T and T-T exchange interactions in these RT_2X_2 compounds, combined with the extensive ranges of solubility of the R, T, and X elements, enables structural and magnetic behaviours to be controlled through elemental substitution.[5–7] Given this scope to tune their physical and magnetic properties and related magnetic phase transitions, RT_2X_2-based compounds have attract attention in exploring their magnetocaloric effect behaviour.[8–10]

We have selected the $NdMn_{2-x}Cr_xSi_2$ system[7] for investigation because the ferromagnetic (F) ordering of Nd sublattice offers scope for simultaneous ferromagnetic ordering of the Mn sublattice, similar to the case in which Fe is substituted for Mn in $Nd(Mn_{1-x}Fe_x)_2Si_2$ system.[11] From this point of view, the replacement of Mn by Cr is expected to significantly modify the magnetic state of both the Nd and the Mn sublattices due to the difference of magnetic moment and atomic radius of Mn (1.35 Å) and Cr (1.30 Å). Based on this ability to design the overall $NdMn_{2-x}Cr_xSi_2$ compounds, we present a detailed investigation of the magnetic phase transitions and entropy change in the layered $NdMn_{1.7}Cr_{0.3}Si_2$ compound.

The polycrystalline $NdMn_{1.7}Cr_{0.3}Si_2$ sample was prepared by arc melting in an Ar atmosphere and annealed at 900 °C for 1 week in an evacuated quartz tube. The samples were characterized by high intensity x-ray powder diffraction ($\lambda = 0.8265$ Å; 10–300 K) carried out at the Australian Synchrotron (AS) and differential scanning calorimetry measurements (DSC; T = 280–430 K). The magnetic properties were investigated over the temperature range of 6–400 K using the vibrating sample magnetometer option of a Quantum Design 14 T physical properties measurement system (PPMS). The crystallographic and magnetic structural behaviour of the sample was investigated by powder neutron diffraction using the Wombat ($\lambda = 2.4205$ Å; 6–400 K) and Echidna ($\lambda = 2.4395$ Å) diffractometers at the OPAL Reactor, Australia.

As shown by the series of x-ray diffraction patterns in Fig. 1(a), the $NdMn_{1.7}Cr_{0.3}Si_2$ compound is single phase and exhibits the body-centered tetragonal $ThCr_2Si_2$-type

[a)]Author to whom correspondence should be addressed. Electronic mail: mfmd999@uowmail.edu.au.

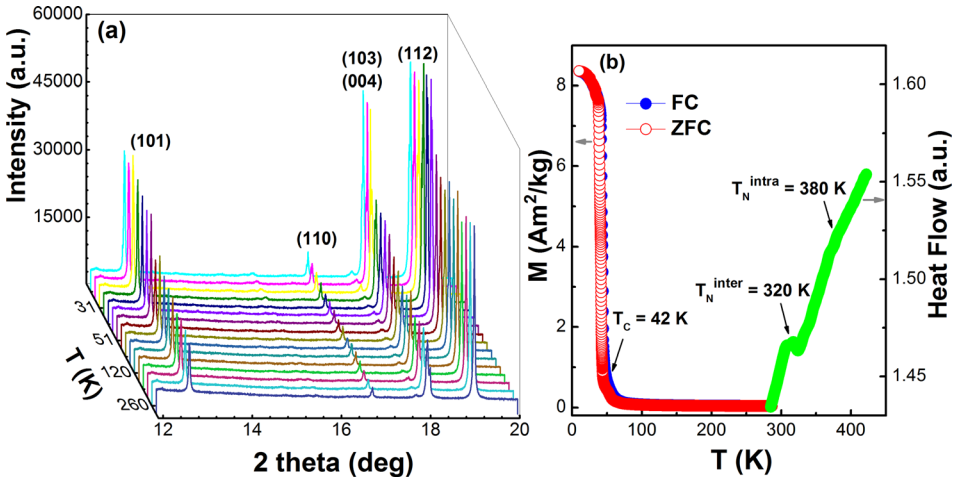

FIG. 1. (a) X-ray diffraction patterns (synchrotron radiation) of $NdMn_{1.7}Cr_{0.3}Si_2$ over the temperature range T = 10–300 K ($\lambda = 0.8265$ Å). (b) Temperature dependence of the magnetization as measured in a field of 0.01 T (left axis: zero field cooling (ZFC) and field cooling (FC)); right axis: DSC results over the range T = 300–420 K).

structure (space group *I*4/*mmm*) over the temperature range of ~10–300 K. No change in crystal structure is observed over this temperature range although, as discussed below, the *a* lattice parameter is found to increase slightly around $T_C \sim 42(2)$ K while the *c* lattice parameter decreases. The patterns have been analysed using FULLPROF[12] software, and the changes in lattices parameters *a* and *c* around T_C (volume change $\Delta V/V \sim 0.1\%$) found to agree well with the neutron data as discussed below.

The temperature dependences of the magnetization of $NdMn_{1.7}Cr_{0.3}Si_2$ (6–295 K) and the differential scanning calorimetry curve obtained at higher temperatures (280–430 K) are shown in Fig. 1(b). As is also evident from the analyses of the neutron diffraction data presented below, $NdMn_{1.7}Cr_{0.3}Si_2$ exhibits three magnetic transitions over the temperature range of 6–400 K. The $T_N^{intra} \sim 380(3)$ K and $T_N^{inter} \sim 320(3)$ K antiferromagnetic transition temperatures were determined from a graph of the DSC data plotted against inverse temperature with the $T_C \sim 42(2)$ K ferromagnetic transition temperature determined from the maximum of the dM/dT versus T curve from the zero-field cooling magnetization data. Comparison of the cooling and warming magnetisation results in Fig. 1(b) shows that the thermal hysteresis at T_C is $\Delta T < \sim 0.8$ K.

Fig. 2(a) shows a thermal contour plot of neutron diffraction measurements on $NdMn_{1.7}Cr_{0.3}Si_2$ from 6 to 400 K. In addition to the set of patterns obtained in the warming ramp mode (step 1 K; counting time 1 min), patterns were obtained around the transition temperatures (5 K steps for 6–70 K; 10 K steps for 80–340 K; 5 K steps for 350–400 K; counting time 10 min). The neutron diffraction patterns in Figs. 3(a)–3(d) are representative of $NdMn_{1.7}Cr_{0.3}Si_2$ in the four regions indicated by the magnetic transition in Fig. 1(b). The different magnetic structures indicated in Fig. 2(b) can be discerned readily from the temperature dependence of the peak intensities for selected magnetic peaks as in Fig. 3(e). The Rietveld refinement of the pattern at 400 K (Fig. 3(a)) confirms that $NdMn_{1.7}Cr_{0.3}Si_2$ has the $ThCr_2Si_2$ structure as expected with the absence of coherent magnetic scattering above $T_N^{intra} \sim 380(3)$ K consistent with paramagnetism. Below $T_N^{intra} \sim 380(3)$ K, $NdMn_{1.7}Cr_{0.3}Si_2$ exhibits the AF*I* antiferromagnetic structure with intralayer coupling (see, e.g., the 375 K pattern of Figs. 3(b) and 3(e) with increased (101) peak intensities) down to $T_N^{inter} \sim 320(3)$ K. On cooling below $T_N^{inter} \sim 320(3)$ K down to T_C, $NdMn_{1.7}Cr_{0.3}Si_2$ exhibits the canted AF*mc* structure (both interlayer and intralayer antiferromagnetic coupling; see, e.g., the 100 K pattern of Fig. 3(c) and related increases in the (101) and (111) peak intensities in Fig. 3(e)). Below T_C, the absence of magnetic scattering from the (111) and (001) reflection at 20 K (Fig. 3(d)), combined with the increase in intensity of the (112) and (101) peaks (Fig. 3(e)), indicate that the interlayer spin components of the Mn moments have a parallel alignment, thus leading to a canted ferromagnetic structure (F*mc*) for

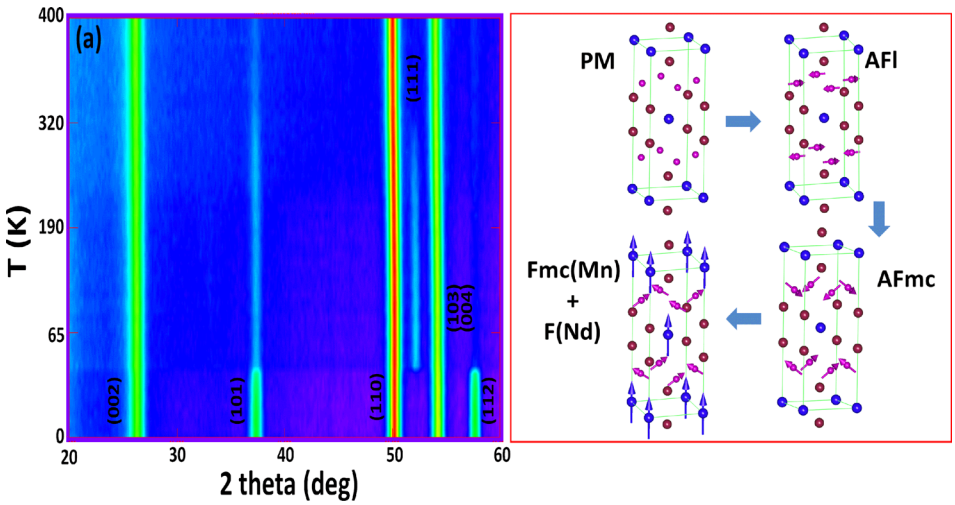

FIG. 2. (a) Neutron diffraction patterns for $NdMn_{1.7}Cr_{0.3}Si_2$ over the temperature range of 6–400 K ($\lambda = 2.4205$ Å). (b) The magnetic structures of $NdMn_{1.7}Cr_{0.3}Si_2$: paramagnetism for $T > T_N^{intra} \sim 380(3)$ K; AF*I* ordering of the Mn sublattice for $T_N^{intra} > T > T_N^{inter} \sim 320(3)$ K; AF*mc* for $T_N^{inter} > T > T_C \sim 42(2)$ K and combined ferromagnetic state F*mc*(Mn) + F(Nd) for $T < T_C$.

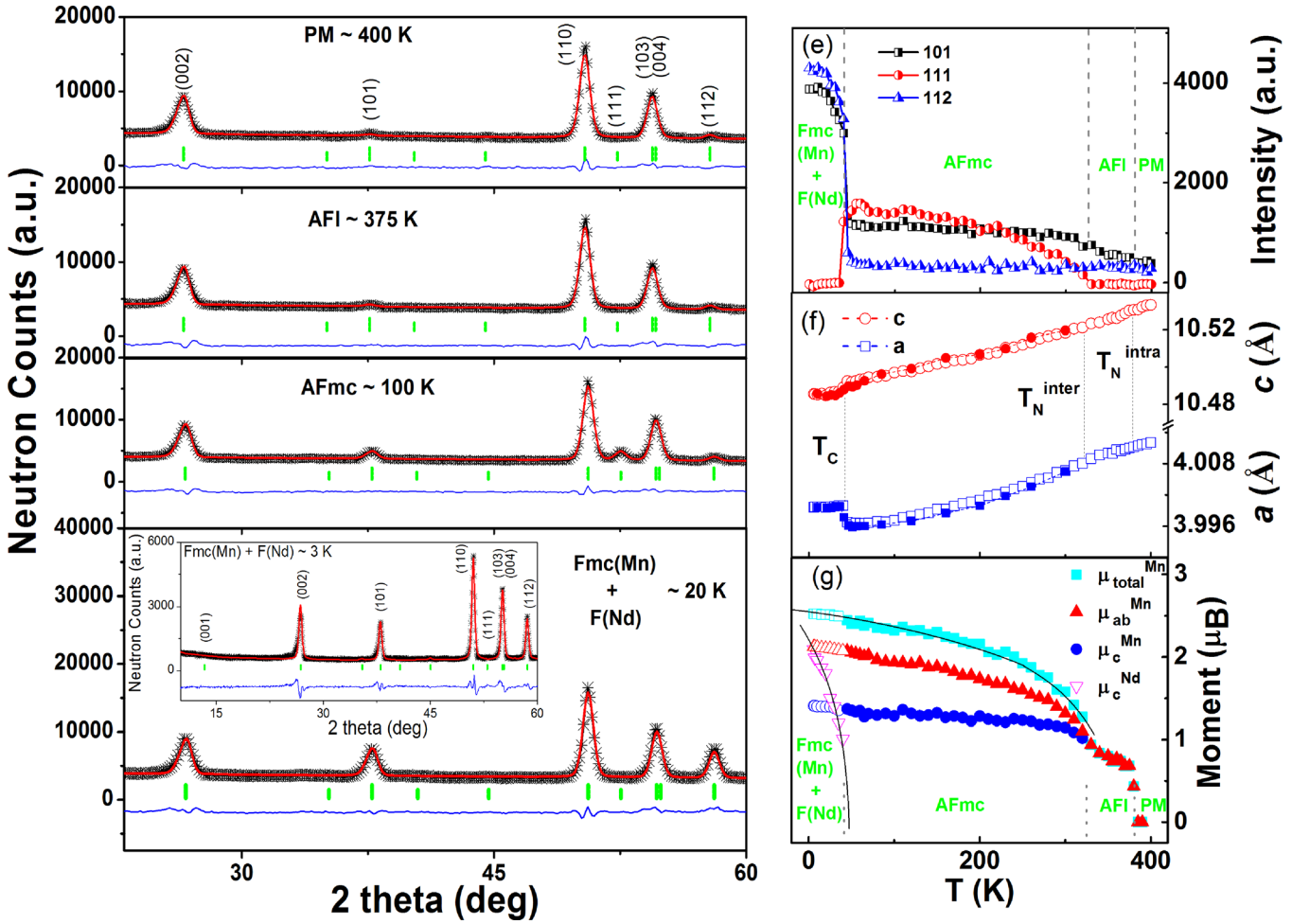

FIG. 3. Neutron diffraction patterns ($\lambda = 2.4205$ Å) for $NdMn_{1.7}Cr_{0.3}Si_2$ at: (a) 400 K; (b) 375 K; (c) 100 K; (d) 20 K (inset-3 K pattern at $\lambda = 2.4395$ Å). (e) Temperature dependence of the integrated intensities of the (101), (111), and (112) reflections; (f) Lattice parameters as a function of temperature (open/closed symbols–neutron/x-ray diffraction). (g) Temperature dependence of the Mn and Nd magnetic moments (6–400 K). The full lines through the open symbols represent the Nd and Mn moments using estimation/fix Mn total moment method as discussed.

the Mn sublattice. The additional high resolution neutron diffraction pattern at T = 3 K (inset to Fig. 3(d)) confirms the absence of the purely magnetic (001) peak and any antiferromagnetic component of the Mn moment in the *ab*-plane below T_C. The further increase in intensities of the (112) and (101) peaks below T_C (Fig. 3(e)) indicates an additional contribution from Nd moments coupled parallel to the Mn moments along the *c*-axis, thereby leading to the formation of the F*mc*(Mn) + F(Nd) magnetic structure. The present results agree well with the findings of Chatterji *et al.*,[13] who demonstrated the ordering of the Nd sublattice in $NdMn_2Si_2$ below T_C from inelastic neutron scattering. It should be noted that the F*mc*(Mn) + F(Nd) configuration in $NdMn_{1.7}Cr_{0.3}Si_2$ differs from that of $NdMn_2Si_2$,[14] $NdMn_{1.9}Ti_{0.1}Si_2$,[15] and $NdMn_{1.8}Co_{0.2}Si_2$ (Ref. 16) for which the (001) peak is present.

As shown in Fig. 3(f), both the *a* and *c* lattice parameters exhibit monotonic decreases with temperature in the antiferromagnetic region between $T_N^{intra} \sim 380(3)$ K and $T_N^{inter} \sim 320(3)$ K, down to $T_C \sim 42(2)$ K. Below $T_C \sim 42(2)$ K, the *a* lattice parameter expands slightly from 3.996(4) Å at 45 K (AF*mc*) to 3.999(5) Å at 6 K (F*mc*(Mn) + F(Nd)), whereas the *c* lattice parameter decreases from 10.492(6) Å to 10.485(5) Å. Good agreement is found with the results of the synchrotron radiation experiments (closed symbols in Fig. 3(f)). The anomalous changes in lattice parameter around $T_C \sim 42(2)$ K indicates the presence of strong magnetostructural coupling.

Fig. 3(g) is a plot of the variation of the Mn magnetic moments with temperature as derived from the refinements. Within the AF*l* and AF*mc* antiferromagnetic regions, the Mn total moment increases from $\mu_{total}^{Mn} = 0.82(4)$ μ_B at $T_N^{inter} \sim 320$ K to $\mu_{total}^{Mn} = 2.04(5)$ μ_B at $T_C \sim 42(2)$ K due to the fact that, with decreasing temperature, thermal disorder becomes weaker compared with magnetic interaction. The sudden rise of Mn moment around T_N^{inter} is due to the appearance of *c*-axis components of Mn moment. Below T_C, $NdMn_{1.7}Cr_{0.3}Si_2$ has the magnetic structure shown in Fig. 2(b). The contributions of the Mn and Nd moments to the ferromagnetic peaks of the neutron diffraction patterns cannot be separated as the magnetic contributions to the *(hkl)* lines from the rare-earth and Mn sublattices overlap below T_C^{Nd} (based on the absence of the (001) peak—see Figure 3(d)). We have therefore extrapolated the temperature dependence of Mn moments above T_C^{Nd} to lower temperatures below T_C^{Nd} (see, e.g., Ref. 17) where both Nd and Mn order in F*mc*(Mn) + F(Nd) region. This leads to the temperature dependence of the Nd moments as shown by the full line in

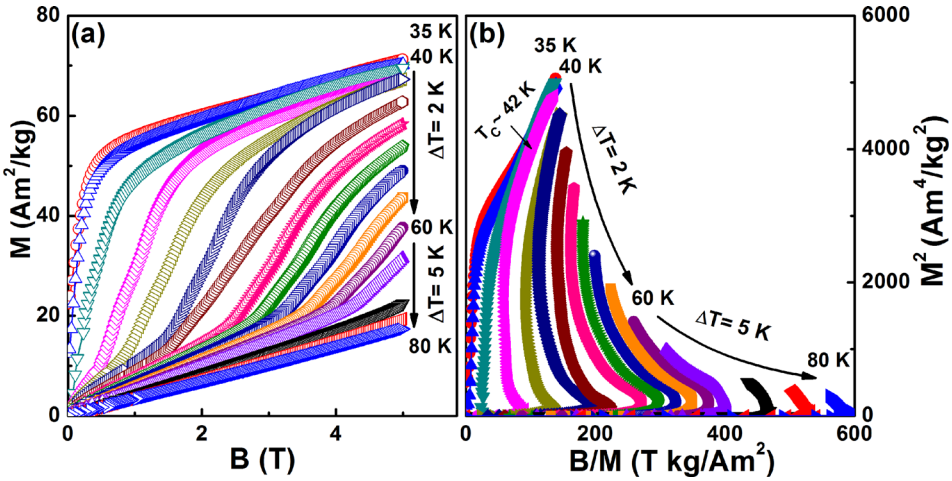

FIG. 4. (a) Magnetization curves for $NdMn_{1.7}Cr_{0.3}Si_2$ over the temperature range of 35–80 K for increasing (closed symbols) and decreasing (open symbols) and (b) the corresponding Arrott plots of M^2 versus B/M.

Fig. 3(g), leading to moment values $\mu_{total}^{Mn} = 2.52(3)\ \mu_B$ and $\mu_c^{Nd} = 2.10(4)\ \mu_B$ at 6 K.

Comparison of the magnetization curves of $NdMn_{1.7}Cr_{0.3}Si_2$ for both increasing and decreasing fields at 2 K intervals over the temperature region ~35–80 K (Fig. 4(a)) demonstrate that there are effectively negligible magnetic hysteresis effects (<~0.1 T) in this compound. This behaviour indicates that $NdMn_{1.7}Cr_{0.3}Si_2$ has promising performance advantages when cycled over the metamagnetic transition from the antiferromagnetic to the ferromagnetic state for magnetic refrigerator applications.[18] As shown by the Arrott plots in Fig. 4(b) and in agreement with the magnetic structures determined from the neutron data as above, $NdMn_{1.7}Cr_{0.3}Si_2$ is ferromagnetic below 42 K (positive intercept on M^2 axis) and antiferromagnetic above 42 K (negative intercept on M^2 axis).[19] The observed negative slope and the S-shaped nature of the Arrott plots characterize a first order magnetic transition. The absence of thermal (<~0.8 K; Fig. 1(b)) and magnetic hysteresis effects (<~0.1 T; Fig. 4(a)) in $NdMn_{1.7}Cr_{0.3}Si_2$ at $T_C \sim 42(2)$ K, compares favourably with other materials such as $Gd_5Si_2Ge_2$ (magnetic hysteresis of ~1 T and thermal hysteresis of ~2 K at $T_C \sim 276$ K)[20] and $La_{0.7}Pr_{0.3}Fe_{11.4}Si_{0.6}$ (magnetic hysteresis of ~0.08 T and thermal hysteresis of ~1.5 K at $T_C \sim 180$ K).[2]

As shown by the magnetic entropy changes in Fig. 5(a) (derived from the magnetization curves using the standard Maxwell relation:[21] $-\Delta S_M(T,B) = \int_0^B \left(\frac{\partial M}{\partial T}\right)_B dB$), the $-\Delta S_M$ peak for $\Delta B = 0-5$ T gradually broadens towards higher temperatures with increasing magnetic field, which is characteristic of a field induced transition from an antiferromagnetic to a ferromagnetic state. The entropy value at the respective Curie temperatures, $-\Delta S_M \sim 15.3$ J kg^{-1} K^{-1} at $T_C \sim 42(2)$ K ($\Delta B = 0-5$ T) for $NdMn_{1.7}Cr_{0.3}Si_2$, is greater than for Gd (9.5 J kg^{-1} K^{-1}) and near that for the giant magnetocaloric effect $Gd_5Si_2Ge_2$ compound (18.8 J kg^{-1} K^{-1}).[20] The MCE value of $NdMn_{1.7}Cr_{0.3}Si_2$ is comparable to those of other materials, which include: GdCoAl[22] ($-\Delta S_M = 10.4$ J kg^{-1} K^{-1} at 100 K) and TbCoAl[22] ($-\Delta S_M = 10.5$ J kg^{-1} K^{-1} at 70 K), all of which, in common with $NdMn_{1.7}Cr_{0.3}Si_2$, importantly exhibit negligible field and thermal hysteresis losses.

The magnetic entropy change, $-\Delta S_M(T, B)$, has also been derived from heat calorimetric measurements of the

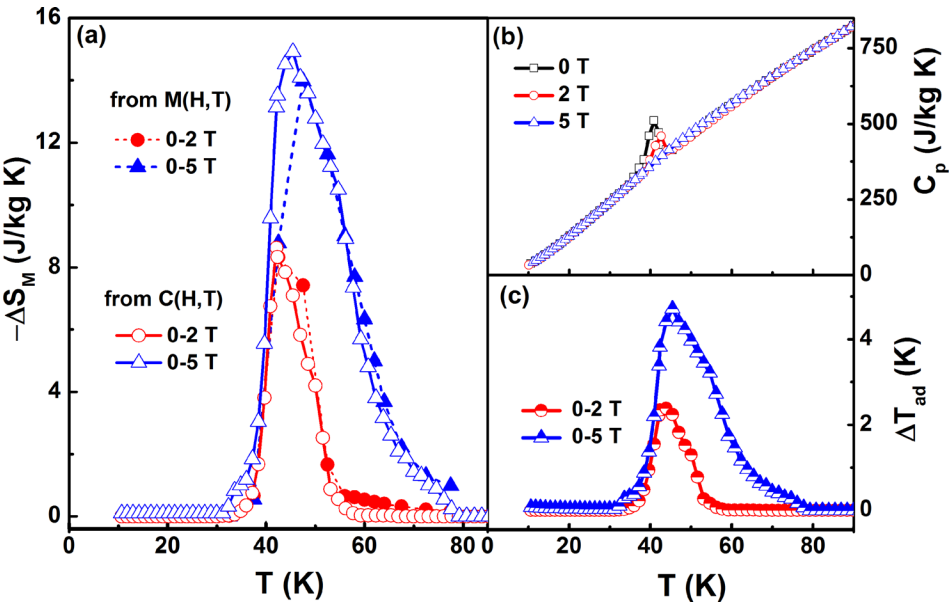

FIG. 5. (a) Magnetic entropy change, $-\Delta S_M$, of $NdMn_{1.7}Cr_{0.3}Si_2$ determined from heat capacity (open symbols) and magnetization (closed symbols) measurements for $\Delta B = 0$-2 T and $\Delta B = 0$-5 T; (b) Heat capacity of $NdMn_{1.7}Cr_{0.3}Si_2$ for B = 0 T, 2 T, 5 T; (c) Adiabatic temperature change, ΔT_{ad}, as determined from the heat capacity measurements of Fig. 5(b).

field dependence of the heat capacity using the expression:[23,24] $-\Delta S_M(T,B) = \int_0^T \left(\frac{C(T,B)-C(T,0)}{T}\right) dT$, where $C(T,B)$ and $C(T,0)$ are the values of the heat capacity measured in field B and zero field, respectively. The corresponding adiabatic temperature change, ΔT_{ad}, can be evaluated from $-\Delta S_M(T, B)$ and the zero field heat capacity data as: $\Delta T_{ad}(T,B) = \int_0^B \frac{T}{C_{B,P}} \left(\frac{\partial M}{\partial T}\right)_B dB$. Fig. 5(b) shows the set of heat capacity measurements obtained for $NdMn_{1.7}Cr_{0.3}Si_2$ (B = 0 T, 2 T, and 5 T) with the corresponding $-\Delta S_M(T, B)$ and ΔT_{ad} values shown in Figs. 5(a) and 5(c). The peak value of the adiabatic temperature change is $\Delta T_{ad}^{max} \sim 5$ K for $\Delta B = 0$-5 T. As shown in Fig. 5(a), the maximum magnetic entropy change determined from the heat capacity measurements of $-\Delta S_M{}^{max} \sim 15$ J kg^{-1} K^{-1} is similar to the value $-\Delta S_M{}^{max} \sim 15.3$ J kg^{-1} K^{-1} determined from the magnetic measurements. This good agreement confirms that the $-\Delta S_M$ values derived for $NdMn_{1.7}Cr_{0.3}Si_2$ from the magnetization measurements represent the MCE behaviour within experimental errors.[20,25] The contribution to the MCE value for $\Delta B = 0-5$ T due to the structural volume expansion is around $-\Delta S_{structural} \sim 1.25$ J kg^{-1} K^{-1} as estimated using the method described by Gschneidner *et al.*[26]

In summary, the magnetic structures of $NdMn_{1.7}Cr_{0.3}Si_2$ determined from variable temperature neutron diffraction studies are: layered AF*l* antiferromagnetism for $T_N{}^{inter} \sim 320(3)$ K < T < $T_N{}^{intra} \sim 380(3)$ K; canted AF*mc* antiferromagnetism for $T_C \sim 42(2)$ K < T < $T_N{}^{inter} \sim 320(3)$ K with a combined F*mc*(Mn) + F(Nd) ferromagnetic structure for $T < T_C \sim 42(2)$ K. Values of the magnetic entropy, magnetocaloric effect and adiabatic temperature change have been determined from magnetization and heat capacity measurements around the first order magnetic transition at T_C. The absence of thermal and magnetic hysteresis in $NdMn_{1.7}Cr_{0.3}Si_2$ at T_C combined with the magnetocaloric values: $-\Delta S_M{}^{max} \sim 15.3$ J kg^{-1} K^{-1} and $\Delta T_{ad}^{max} \sim 5$ K under $\Delta B = 0$-5 T, indicate scope for $NdMn_{1.7}Cr_{0.3}Si_2$ as an active magnetic refrigerator, especially for the helium liquefaction environment.

This work was supported in part by Australian Research Council Discovery Projects (DP0879070 and DP110102386). M.F.M.D. acknowledges the Ministry of Higher Education, Malaysia, for a postgraduate research scholarship.

[1]K. A. Gschneidner, Jr., V. K. Pecharsky, and A. O. Tsokol, Rep. Prog. Phys. **68**, 1479 (2005).
[2]M. F. Md Din, J. L. Wang, R. Zeng, P. Shamba, J. C. Debnath, and S. X. Dou, Intermetallics **36**, 1 (2013).
[3]M. Hofmann, S. J. Campbell, and A. V. J. Edge, Phys. Rev. B **69**, 174432 (2004).
[4]E. G. Gerasimov, N. V. Mushnikov, and T. Goto, Phys. Rev. B **72**, 064446 (2005).
[5]G. Venturini, R. Welter, E. Ressouche, and B. Malaman, J. Magn. Magn. Mater. **150**, 197 (1995).
[6]J. L. Wang, L. Caron, S. J. Campbell, S. J. Kennedy, M. Hofmann, Z. X. Cheng, M. F. Md Din, A. J. Studer, E. Brück, and S. X. Dou, Phys. Rev. Lett. **110**, 217211 (2013).
[7]R. Obermyer, S. G. Sankar, and V. U. S. Rao, J. Appl. Phys. **50**, 2312 (1979).
[8]J. L. Wang, S. J. Campbell, A. J. Studer, M. Avdeev, R. Zeng, and S. X. Dou, J. Phys.: Condens. Matter **21**, 124217 (2009).
[9]J. L. Wang, S. J. Campbell, R. Zeng, C. K. Poh, S. X. Dou, and S. J. Kennedy, J. Appl. Phys. **105**, 07A909 (2009).
[10]R. Zeng, S. X. Dou, J. L. Wang, and S. J. Campbell, J. Alloys Compd. **509**, L119 (2011).
[11]Y. Q. Chen, J. Luo, J. K. Liang, J. B. Li, and G. H. Rao, Chin. Phys. B **18**, 4944 (2009).
[12]L. B. McCusker, R. B. Von Dreele, D. E. Cox, D. Louër, and P. Scardi, J. Appl. Crystallogr. **32**, 36 (1999).
[13]T. Chatterji, J. Combet, B. Frick, and A. Szyula, J. Magn. Magn. Mater. **324**, 1030 (2012).
[14]R. Welter, G. Venturini, D. Fruchart, and B. Malaman, J. Alloys Compd. **191**, 263 (1993).
[15]M. F. M. Din, J. L. Wang, S. J. Campbell, R. Zeng, W. D. Hutchison, M. Avdeev, S. J. Kennedy, and S. X. Dou, J. Phys. D: Appl. Phys. **46**, 445002 (2013).
[16]S. M. Yusuf, M. Halder, A. K. Rajarajan, A. K. Nigam, and S. Banerjee, J. Appl. Phys. **111**, 093914 (2012).
[17]I. Dincer, A. Elmali, Y. Elerman, H. Ehrenberg, H. Fuess, and O. Isnard, J. Phys.: Condens. Matter **16**, 2081 (2004).
[18]U. Plaznik, J. Tušek, A. Kitanovski, and A. Poredoš, Appl. Therm. Eng. **59**, 52 (2013).
[19]R. Zeng, J. L. Wang, L. Lu, W. X. Li, S. J. Campbell, and S. X. Dou, J. Alloys Compd. **505**, L38 (2010).
[20]V. K. Pecharsky and J. K. A. Gschneidner, Phys. Rev. Lett. **78**, 4494 (1997).
[21]H. Feng-Xia, S. Bao-Gen, S. Ji-Rong, C. Zhao-Hua, and Z. Xi-Xiang, J. Phys.: Condens. Matter **12**, L691 (2000).
[22]X. X. Zhang, F. W. Wang, and G. H. Wen, J. Phys.: Condens. Matter **13**, L747 (2001).
[23]V. K. Pecharsky and J. K. A. Gschneidner, J. Appl. Phys. **86**, 565 (1999).
[24]B. Ekkes, J. Phys. D: Appl. Phys. **38**, R381 (2005).
[25]J. L. Wang, S. J. Campbell, J. M. Cadogan, A. J. Studer, R. Zeng, and S. X. Dou, Appl. Phys. Lett. **98**, 232509 (2011).
[26]K. A. Gschneidner, Jr., Y. Mudryk, and V. K. Pecharsky, Scr. Mater. **67**, 572 (2012).